Supplementary Material

Supplementary Figure 1

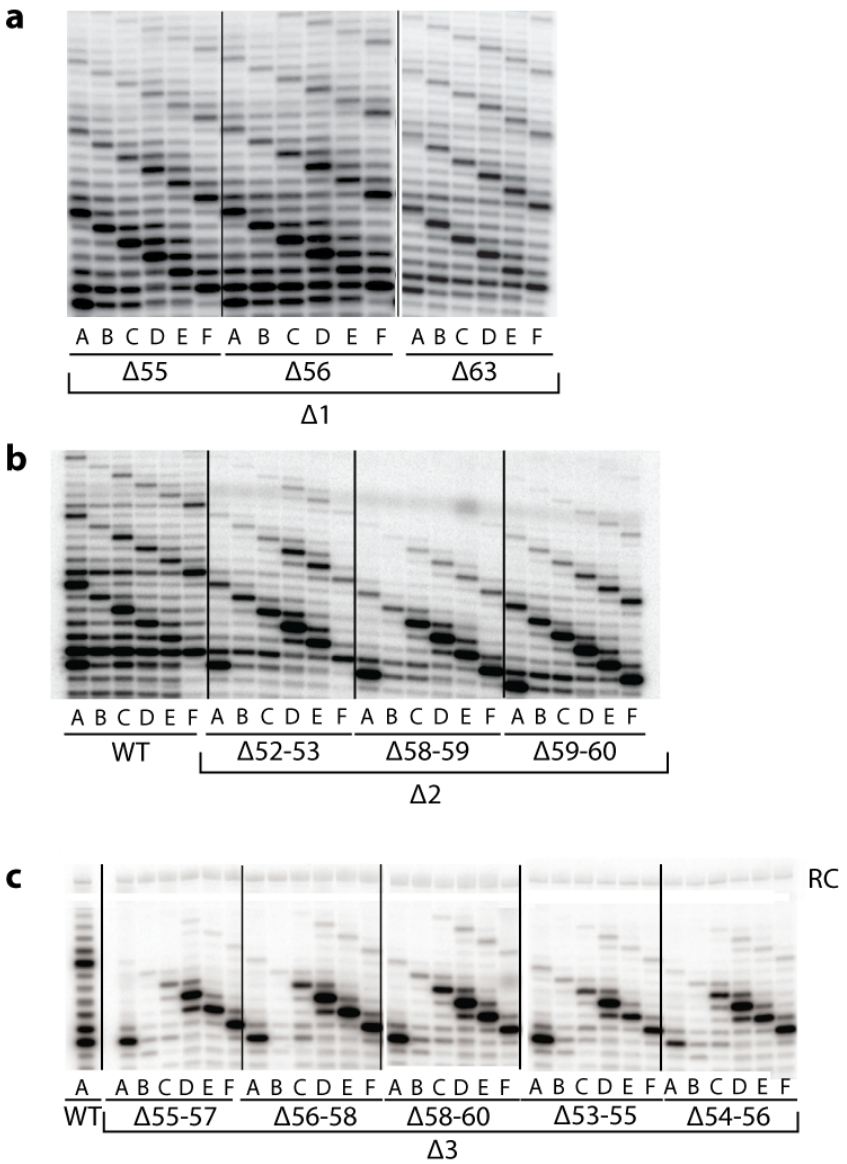

Supplementary Figure 1. Primer profiles of deletion mutants. Telomerase activity assays with the indicated primers for (**a**) single nucleotide deletions, (**b**) double nucleotide deletions and (**c**) triple nucleotide deletions. RC, recovery control.

Supplementary Figure 2

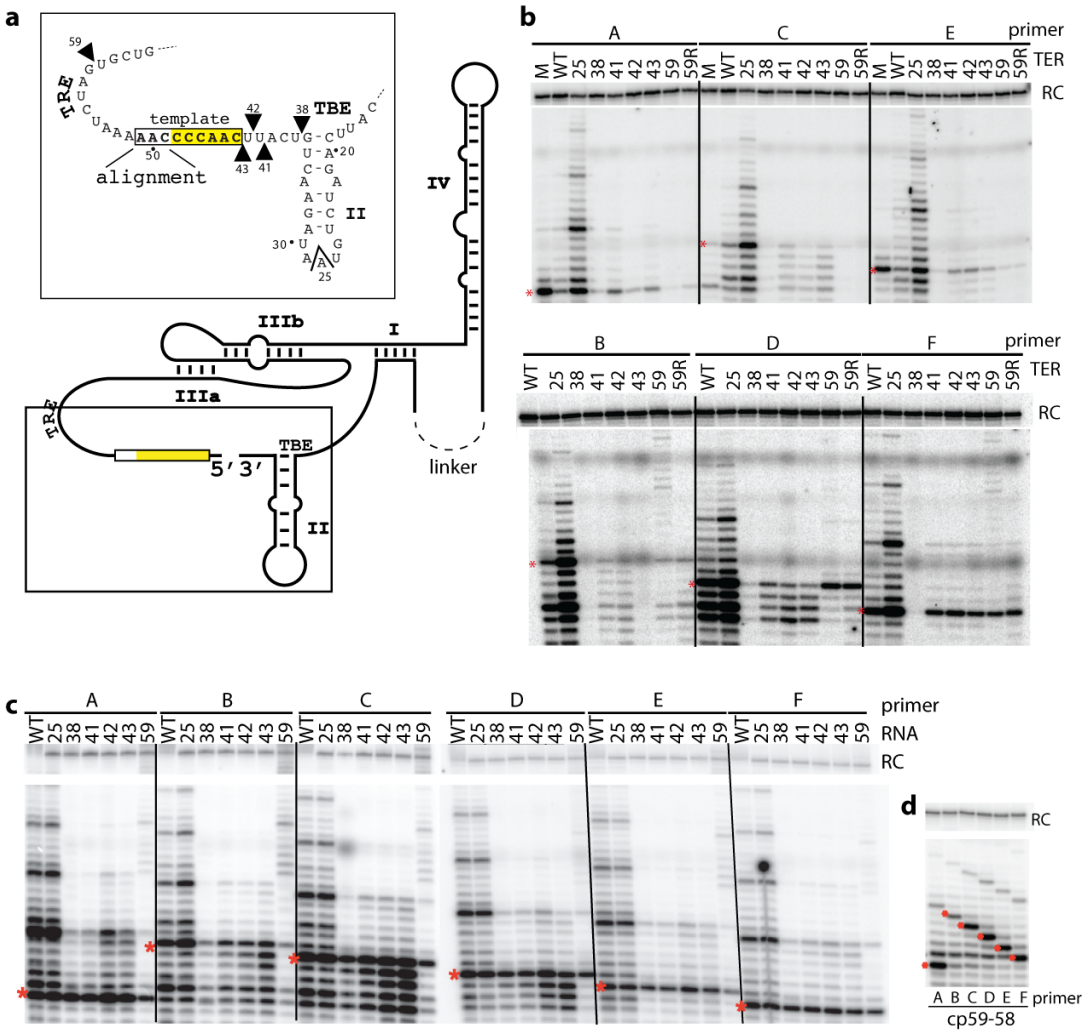

Supplementary Figure 2. Telomerase molecules containing nicks in the TRE or the TBE exhibit minimal telomerase RAP. (**a**) Construction of cpRNAs. The natural 5‘ and 3’ ends were connected by a linker[1] (dashed line). Inset, TER sequence spanning the template in the cpRNAs. The closed triangles indicate where each circular permutation was generated, with the 5’ end of the cpRNA labeled. For example, 42 is a circular permutation with the 5’ end at nucleotide 42 and the 3’ end at nucleotide 41. cp25 begins at nucleotide 31 and ends at nucleotide 25; three GC base pairs terminate this stem for stabilization[1]. (**b**) Telomerase activity assays of indicated cpRNAs and WT TER assembled in the (**b**) absence and (**c-d**) presence of p65. (**d**) Telomerase activity assays on telomerase containing cp59-58 RNA that were treated during the last five minutes of the assay with RNase A. Primers are indicated below each lane. Asterisks, first round of repeat synthesis for each primer. RC, recovery control.

Supplementary Figure 3

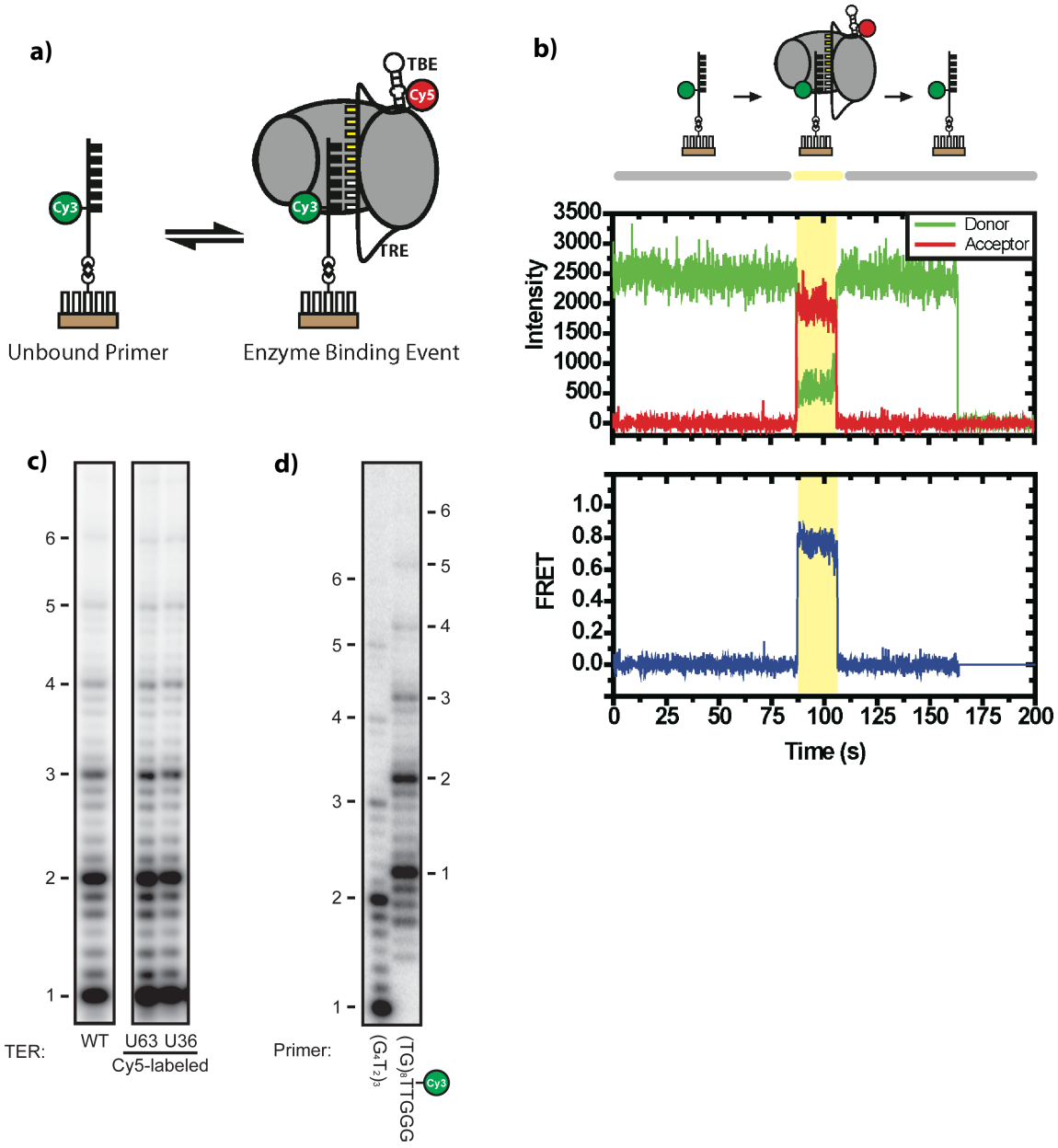

Supplementary Figure 3. Real-time detection of telomerase-DNA interactions by single molecule FRET. (**a**) Surface-immobilized telomeric DNA primers labeled at the n-2 alignment position with a FRET donor dye (Cy3) are incubated in the presence of telomerase enzymes labeled with an acceptor dye (Cy5) within the telomerase RNA. (**b**) Binding of the Cy5-labeled telomerase to the surface immobilized Cy3-labeled DNA primer

gives rise to FRET, characterized by the anti-correlated change in donor (green) and acceptor (red) dye intensities (top panel). The sudden drop in donor intensity at the end of the single molecule trace is due to irreversible photobleaching of the dye. FRET was calculated as described in the Methods section. (**c**) Telomerase activity assays were performed on telomerase enzymes reconstituted with unmodified *in vitro* transcribed TER (WT) or with TER labeled at either U63 or U36 with Cy5. The telomerase activity assays demonstrate that fluorophore modification at these two sites has no effect on telomerase processivity. Numbers indicate how many telomeric repeats have been added at each band. (**d**) Telomerase activity assays were performed either in the presence of a telomeric 18-nt DNA primer $(G_4T_2)_3$ or in the presence of a $(TG)_8$ telomeric repeat primer labeled with Cy3 at the n-2 position. The activity assays reveal that Cy3-labeled $(TG)_8$ primers support a similar level of telomerase activity as the unmodified native telomeric sequence primers. The $(TG)_8$ primer appears higher on the gel due to the combined effect of having three extra nucleotides and the Cy3 modification.

Supplementary Figure 4

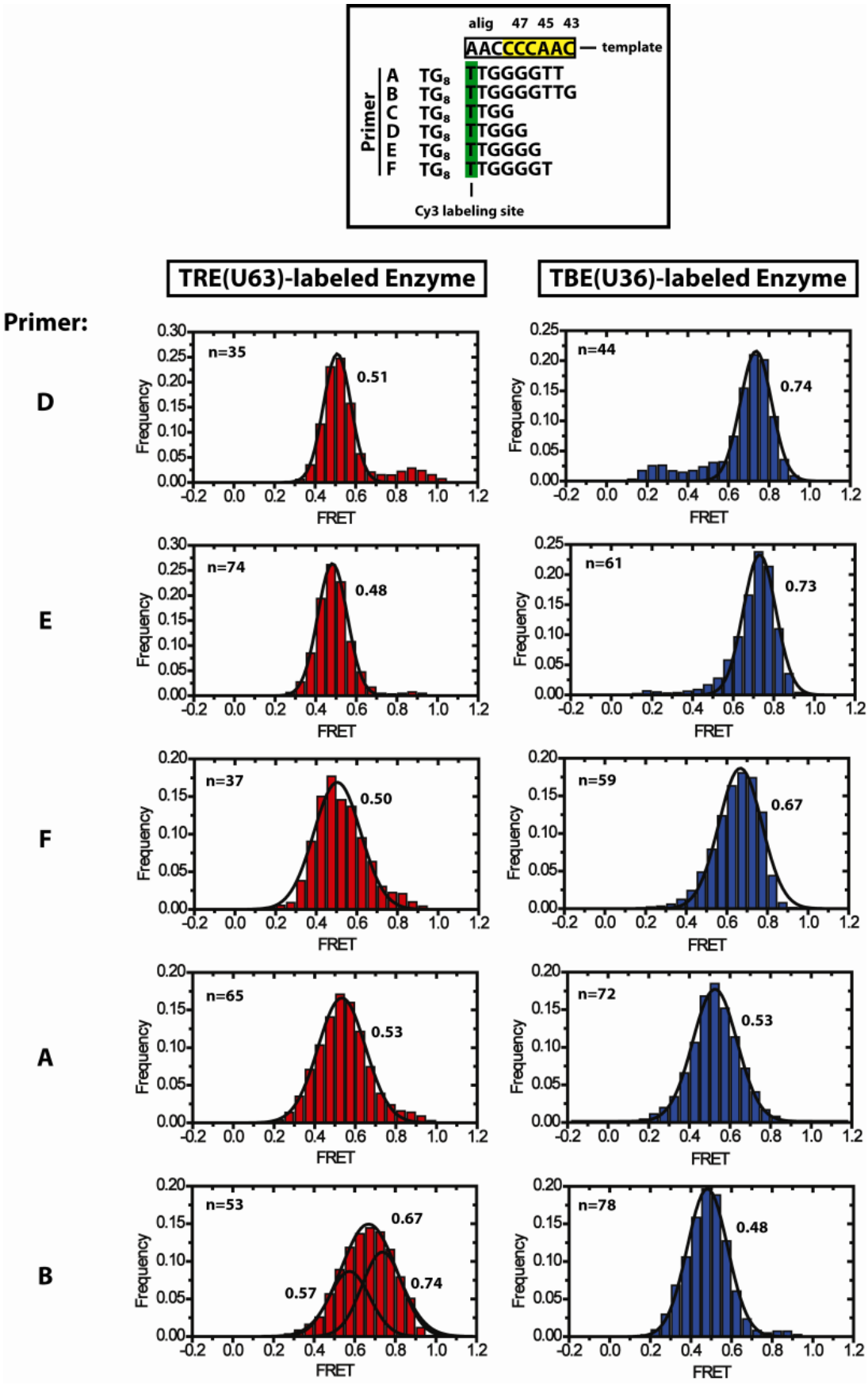

Supplementary Figure 4. Representative single molecule FRET histograms for each telomere DNA primer permutation. smFRET experiments were conducted using DNA primers with a 5' $(TG)_8$ stretch followed by a single copy of various permutations of telomere repeat sequence corresponding to intermediates in the telomere DNA repeat synthesis reaction, as shown in the top panel. Representative histograms for TRE (U63)- and TBE (U36)-labeled enzymes binding to the indicated telomere DNA primers were generated by compiling all observed FRET values for the duration of the indicated number of binding events. Histograms were fit to Gaussian functions to determine the center of the FRET distribution.

Notably, the FRET distributions for both the TRE (U63)- and TBE (U36)-labeled enzyme become gradually broader as the primer length is increased (primers F, A, B), and are not consistent with a single stable FRET distribution. As discussed further in Supplementary figures 5 and 6, the histogram broadening is the result of transient FRET fluctuations for these primers. However, since the physical basis for these FRET dynamics is not understood at present, we chose to fit the data with a single Gaussian to obtain the average FRET behavior for all experiments except the experiment with TRE (U63)-labeled enzyme and primer B, which showed a distinct bimodal distribution of FRET values (see Supplementary Fig. 6, primer B). In this case, the broad FRET distribution was fit with two Gaussian functions rather than one in order to suppress an artificially large increase in the apparent FRET value, which would be observed if we treated the data as a unimodal distribution. Experiments performed with the shortest primer, primer C, yielded very few binding events. In addition they tended to be very short-lived and unstable in their FRET values. As a result, primer C was not used in this study.

Supplementary Figure 5

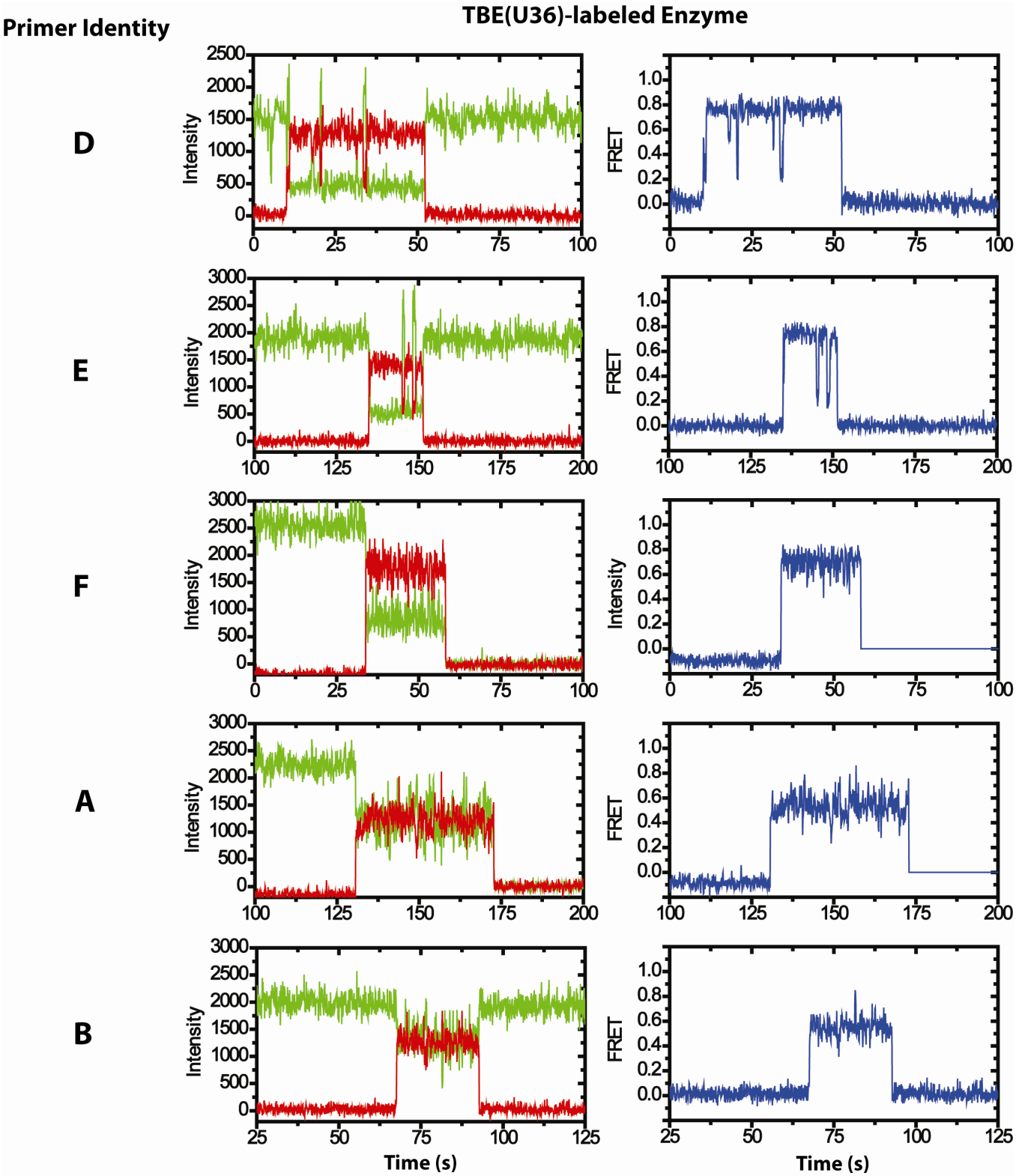

Supplementary Figure 5. Representative single molecule FRET trajectories for TBE (U36)-labeled telomerase. Examples of single molecule traces obtained with each of the indicated primers are shown. The left column shows the donor (green) and acceptor (red) dye intensities and the right column is the calculated FRET ratio after normalization and correction for Cy3 intensity enhancement due to the presence of the protein (see Methods for more details on γ correction). In the case of primer D, transient fluctuations to a lower FRET state ($\sim$0.2) were observed, giving rise to a small additional peak in the FRET histogram (see Supplementary Fig. 4, primer D). The origin of these FRET dynamics is not known at present. One possibility is that this low FRET state represents a complex in which the DNA primer is only bound at the previously described anchor site, which comprises an interaction surface that is independent of the enzyme active site. As the primer length is increased, we observe oscillations in individual FRET traces consistent with a broadening observed in the histograms for these primers (see Supplementary Fig. 4). In some cases, these FRET fluctuations could be clearly resolved as anti-correlated donor and acceptor dye intensities, suggesting the increase in FRET dynamics likely represents a transient rearrangement of the FRET probes. These fluctuations may represent functionally important structural dynamics of the telomere DNA primer, telomerase RNA, or both; however, a precise description of the physical basis for the observed FRET dynamics awaits further investigation.

Supplementary Figure 6

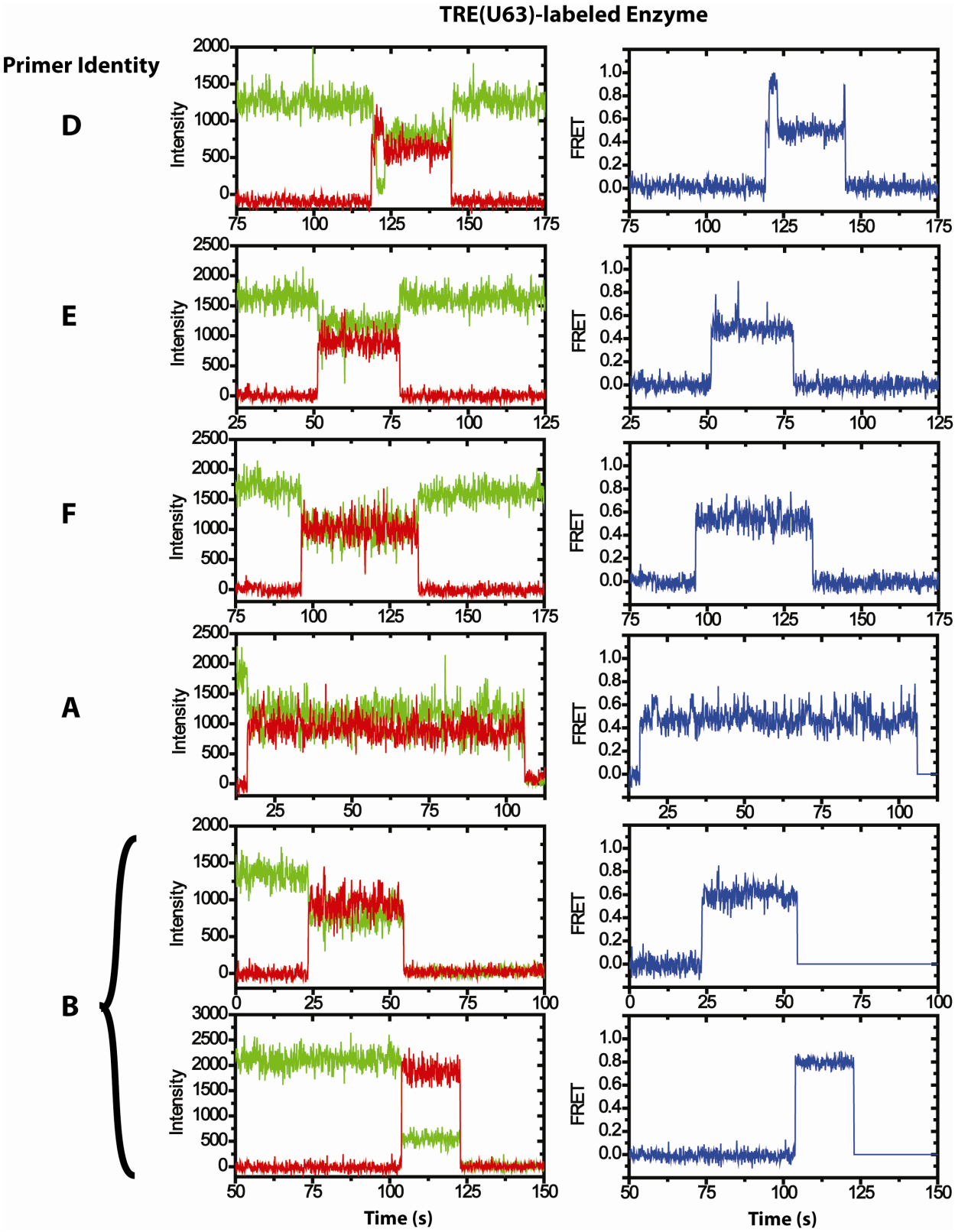

Supplementary Figure 6. Representative single molecule FRET trajectories for TRE (U63)-labeled telomerase. Examples of single molecule traces obtained with each of the indicated primers are shown. The left column shows the donor (green) and acceptor (red) dye intensities and the right column is the calculated FRET ratio after normalization and correction for Cy3 intensity enhancement due to the presence of the protein (see Methods for more details on γ correction). As described in Supplementary Fig. 5, experiments performed with primer D showed a predominantly stable FRET level interrupted by transient FRET transitions. In the case of the TRE (U63)-labeled enzyme, we observed transient excursions to a higher FRET value, giving rise to a small peak at FRET ~0.9 in the FRET histograms (see Supplementary Fig. 4, primer D). Interestingly, the direction of these transient FRET dynamics is anti-symmetric for the TRE (U63)- and TBE (U36)-labeled enzymes, suggesting the signal is derived from a rearrangement of the DNA primer that brings the Cy3 label closer to the TRE and further from the TBE, consistent with a primer binding mode in which only the DNA anchor site (located near the TRE) is occupied. As was seen for the TBE (U36)-labeled enzyme, we again observed a gradual increase in the amplitude of the FRET fluctuations with longer DNA primers (primers F, A, and B). In a subset of the traces, these fluctuations were clearly resolved as anti-correlated donor and acceptor dye intensities, suggesting they are the result of a dynamic reorientation of the FRET probes, rather than a photo-physical artifact.

Notably, in the case of the TRE (U63)-labeled enzyme and DNA primer B, in addition to the trend of increased FRET dynamics around 0.5-0.6 FRET, we also observed a substantial number of single molecule traces showing a very stable high FRET behavior (FRET~0.75). The observation of these two sub-populations could be explained by the fact that primer B, which corresponds to a complete telomere DNA repeat, may bind in two distinct registers, one corresponding to the pre-translocated state and the other to the post-translocated state of the enzyme with respect to the primer. Importantly, as stated in the main text, the trend we observe for structural changes in the TRE holds whether we consider either of the two individual FRET states or the average of the two. Curiously, we only observe a single distribution for the TBE (U36) labeling site with primer B (see Supplementary Fig. 5). There are two possible explanations for this observation. One possibility is that the increase in FRET is due to movement of the U63 labeling site closer to a primer that remains in a fixed position in the enzyme. The other possibility is that it is the primer labeling site that moves relative to fixed U63 and U36 labeling sites, however the movement is such that the primer moves closer to the U63 labeling site without changing its net distance to the U36 labeling site.

Supplementary Figure 7

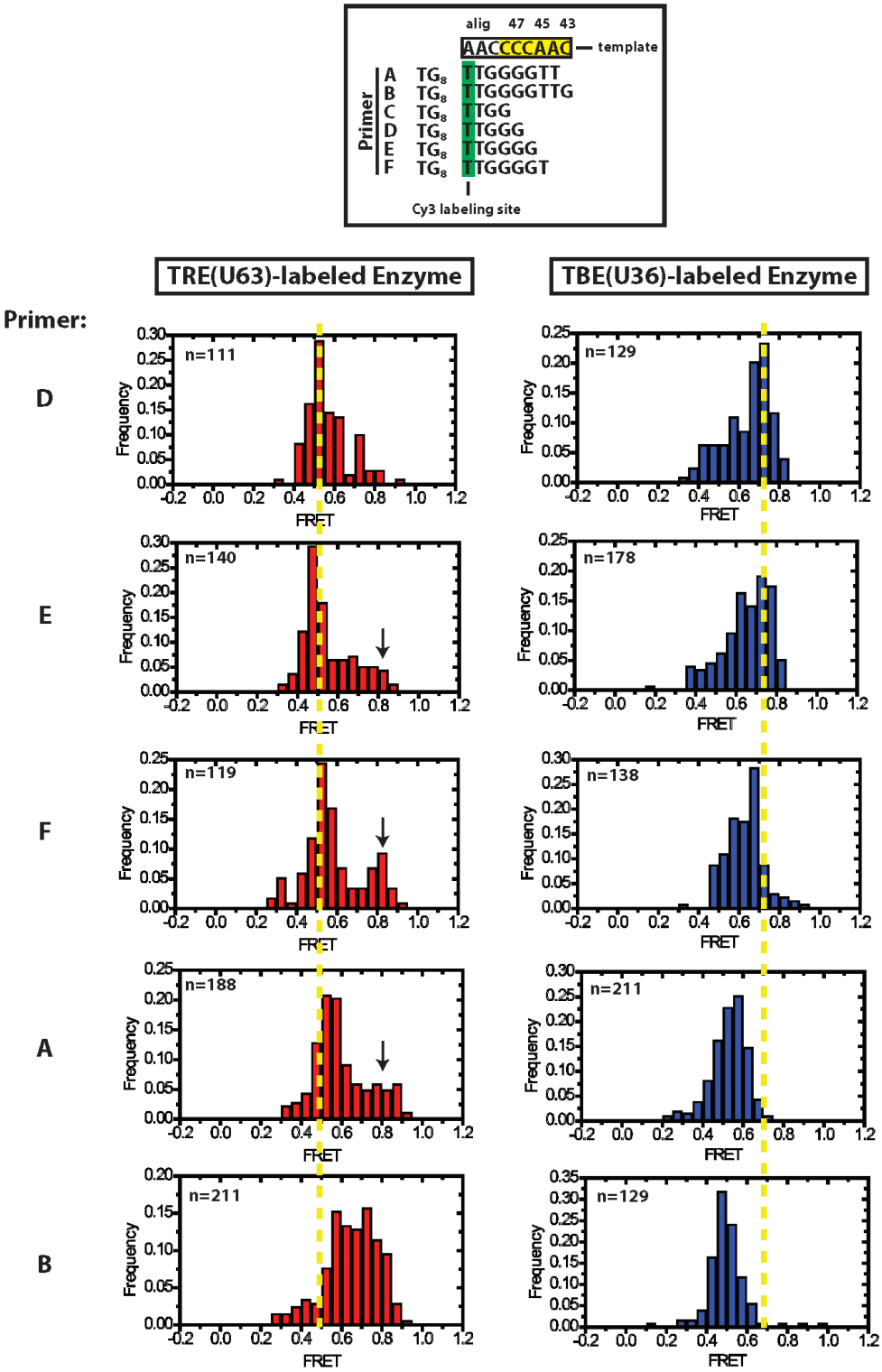

Supplementary Figure 7. Mean FRET histograms for each telomere DNA primer permutation. As an alternative way to represent the FRET data, we took the mean FRET value for each individual binding event and binned these values into mean FRET histograms. Since this approach yields fewer data points, we combined all binding events for each enzyme-primer combination from each of the experiments performed in triplicate to generate the mean FRET histograms. Importantly, the trends in the FRET values for the dominant populations observed in our experiments are similar in the mean FRET histograms and the total FRET histograms (see Supplementary Fig. 4). It is evident from these histograms that for both the TRE (U63)- and TBE (U36)-labeled enzymes, there are short-lived binding events that are not represented in the total FRET histograms (black arrows). In the case of the TRE (U63)-labeled enzyme and primer B, the number and duration of the high FRET binding events is substantially increased, consistent with the observation of a large number of traces exhibiting a stable high FRET behavior (see Supplementary Fig. 6). Importantly, we observe the same trends in the mean FRET histograms as we observe in the histograms of total events (see Supplementary Fig. 4), as indicated by the positions of the distributions relative to the yellow dashed lines.

Supplementary Figure 8

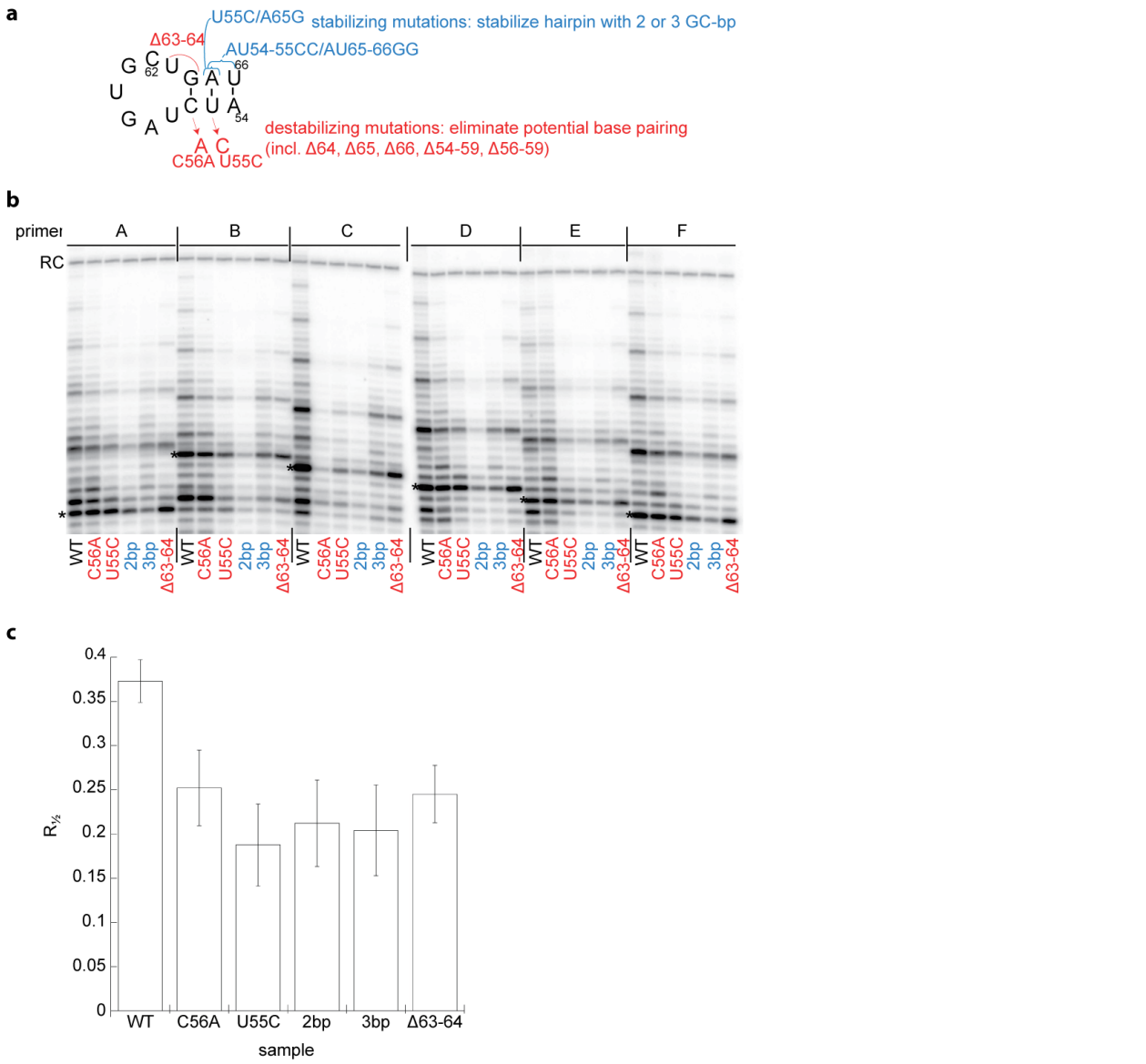

Supplementary Figure 8. Alternative hairpin model for template progression through the active site. (**a**) Diagram of potential hairpin that might form in the TRE. Mutations were generated that would be predicted to either stabilize (blue) or destabilize (red) the putative hairpin. (**b**), Telomerase activity assays for telomerase RNPs containing each indicated mutant. Asterisks indicate the first nucleotide added to each primer. RC, recovery control. (**c**) Quantitation of the gel in panel **b.** Error bars are the standard deviation over six primers (n=6). Processivity is represented as $R_{1/2}$, a number that summarizes the percent of primers that have been extended by the telomerase RNP past a given repeat[2].

References for Supplementary Material

1. Miller, M.C. & Collins, K. Telomerase recognizes its template by using an adjacent RNA motif. *Proceedings of the National Academy of Sciences of the United States of America* **99**, 6585-90 (2002).
2. Latrick, C.M. & Cech, T.R. POT1-TPP1 enhances telomerase processivity by slowing primer dissociation and aiding translocation. *The EMBO Journal* **29**, 924-33 (2010).